Supporting Information

Rinne et al. 10.1073/pnas.1212656110

SI Methods

Fluorescence Microscopy and Electrophysiology. FRET signals between CFP and YFP were recorded from single cells using an inverted microscope (Axiovert 135; Carl Zeiss) equipped with an oil-immersion objective (A-plan 100×/1.25, Carl Zeiss), a Polychrome V light source, and a dual-emission photometry system (both TILL Photonics). CFP was excited with brief light flashes (duration, 5 ms; frequency, 1 or 5 Hz) at $\lambda = 425$ nm to limit photobleaching (excitation filter: ET436/20, beamsplitter: DCLP460). Emitted donor fluorescence (F_{480}) and acceptor fluorescence (F_{535}) were collected with photodiodes (beam-splitter: DCLP505; emission filters D480/40 and HQ535/30, respectively) and digitalized with a computer interface (ITC16; HEKA Elektronik). Individual traces representing F_{535} and F_{480} were acquired at 1- or 5-Hz sampling rate and displayed on a personal computer using Patchmaster software (v2X52; HEKA). FRET was calculated as ratio F_{535}/F_{480} (termed FRET ratio) and corrected for photobleaching (Fig. S1). All beam-splitters or filters were from Chroma Technology.

Patch pipettes of 3 MΩ to 5 MΩ resistance were obtained using borosilicate glass capillaries (GL150F-10; Harvard Apparatus) with a horizontal pipette puller (P87; Sutter Instruments). Measurements were performed using the whole-cell configuration and cells were clamped to a holding potential (V_{hold}) of −90 mV or various test potentials with an EPC-7 amplifier (HEKA) in the voltage-clamp mode. Whole-cell G protein-activated inwardly rectifying K^+ (GIRK) currents were recorded at room temperature in the inward direction (V_{hold}: −40 mV or −100 mV, $E_K = 0$ mV) (Fig. S2). Recording of inward currents was chosen over measuring outward currents, because the degree of inward rectification (limiting outward current amplitudes) depends on the amount of activated G proteins, and is therefore different between low- and high-agonist concentrations at positive membrane potentials. In contrast, current amplitudes that are measured in the inward direction are not affected by this phenomenon (1). During experiments, cells were continuously superfused with extracellular buffer or agonist-containing solution (see below) using a pressurized perfusion system (ALA Scientific Instruments) that allows for rapid (< 10 ms) exchange of solutions. The membrane potential V_M and application of agonists were controlled and synchronized with Patchmaster software.

Chemicals and Solutions. The extracellular buffer was composed of: NaCl 137 mM, $CaCl_2$ 2 mM, KCl 5.4 mM, $MgCl_2$ 1 mM, Hepes 10 mM (pH = 7.4). Patch pipettes were filled with intracellular solution consisting of: K^+-aspartate 100 mM, KCl 40 mM, NaCl 5 mM, $MgCl_2$ 7 mM, EGTA 10 mM, GTP 0.025 mM, Na^+-ATP 5 mM, Hepes 20 mM (pH = 7.2). After a stable seal was formed and before agonists were applied, cells were superfused with extracellular buffer that was nominally Ca^{2+}-free to prevent Ca^{2+}-activated chloride influx during membrane depolarization, which quenches YFP fluorescence (2, 3). For GIRK current measurements, a high K^+-buffer was used as extracellular solution (as above, but containing 140 mM K^+ and 2.4 mM Na^+). For measurements using GTPγS, a modified pipette solution was used where GTP was replaced with 500 μM GTPγS. Solutions containing norepinephrine (NE) or clonidine were prepared with Ca^{2+}-free buffer. All chemicals were from Sigma-Aldrich or Tocris Bioscience.

Analysis of Charge Movements, Activation Kinetics, and Concentration-Dependent Responses. The voltage-dependence of gating-charge movement was determined by fitting a single Boltzmann function to the normalized degree of receptor activation (R) values (Fig. 1*E*) with Origin 8.1 software (OriginLab). The equation used to fit the data were $R = R_{max}/(1 + \exp[-(V - V_{0.5})/k])$, where R_{max} is the maximal receptor activation, V the membrane potential, $V_{0.5}$ the voltage for half-maximal effect on receptor activation, and k the slope factor. The Boltzmann fit was performed using GraphPad Prism software (v5; GraphPad Prism Software).

To determine the kinetics of receptor activation by agonists or voltage, corresponding time constants τ were calculated by fitting the FRET response of receptor activation (indicated in Fig. 2) to a first-order exponential decay. Curve fitting and calculation of τ-values was performed using Origin 8.1 software.

To obtain concentration-response curves, the FRET amplitudes of α_{2A}AR-cam in response to a given NE concentration were measured at −90 mV and +60 mV and normalized to the corresponding amplitudes of the same cell evoked by 100 μM NE at both potentials ($FRET/FRET_{100\mu M}$), which was defined as maximal response. These normalized amplitudes were then plotted against (NE). Sigmoid curve fitting and calculation of EC_{50} values was performed with GraphPad Prism.

1. Hommers LG, Lohse MJ, Bünemann M (2003) Regulation of the inward rectifying properties of G-protein-activated inwardly rectifying K+ (GIRK) channels by Gβγ subunits. *J Biol Chem* 278(2):1037–1043.
2. Elsliger M-A, Wachter RM, Hanson GT, Kallio K, Remington SJ (1999) Structural and spectral response of green fluorescent protein variants to changes in pH. *Biochemistry* 38(17):5296–5301.
3. Wachter RM, Remington SJ (1999) Sensitivity of the yellow variant of green fluorescent protein to halides and nitrate. *Curr Biol* 9(17):R628–R629.

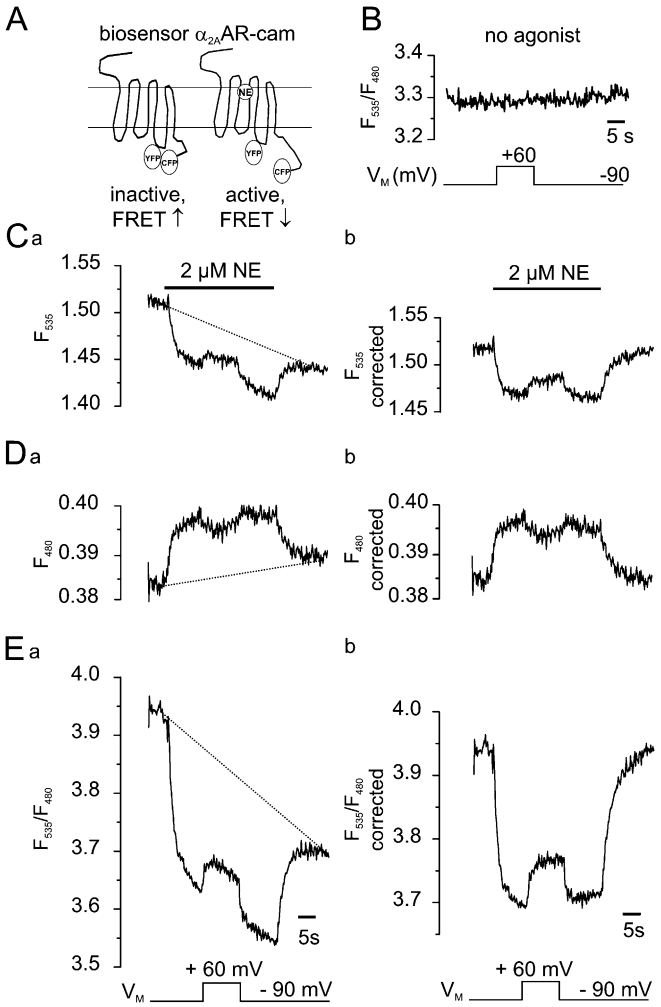

Fig. S1. FRET measurements using α_{2A}AR-cam and correction for photobleaching. (*A*) Schemeatic representation of the biosensor α_{2A}AR-cam. Binding of NE results in activation of the biosensor, reflected as a decrease in the FRET ratio (F_{535}/F_{480}). (*B*) Voltage does not modulate the inactive conformation of the biosensor. (*C–E*) Raw fluorescence traces of F_{535} (YFP; *C*, *a*) and F_{480} (CFP; *D*, *a*). Pronounced bleaching of YFP (dotted line) causes a linear decrease in F_{535} and the FRET ratio (*E*, *a*), accompanied by an increase in F_{480} because of FRET. Subsequent subtraction of this linear decline yields to bleach-corrected values of F_{535} (*C*, *b*), F_{480} (*D*, *b*), and the FRET ratio F_{535}/F_{485} (*E*, *b*).

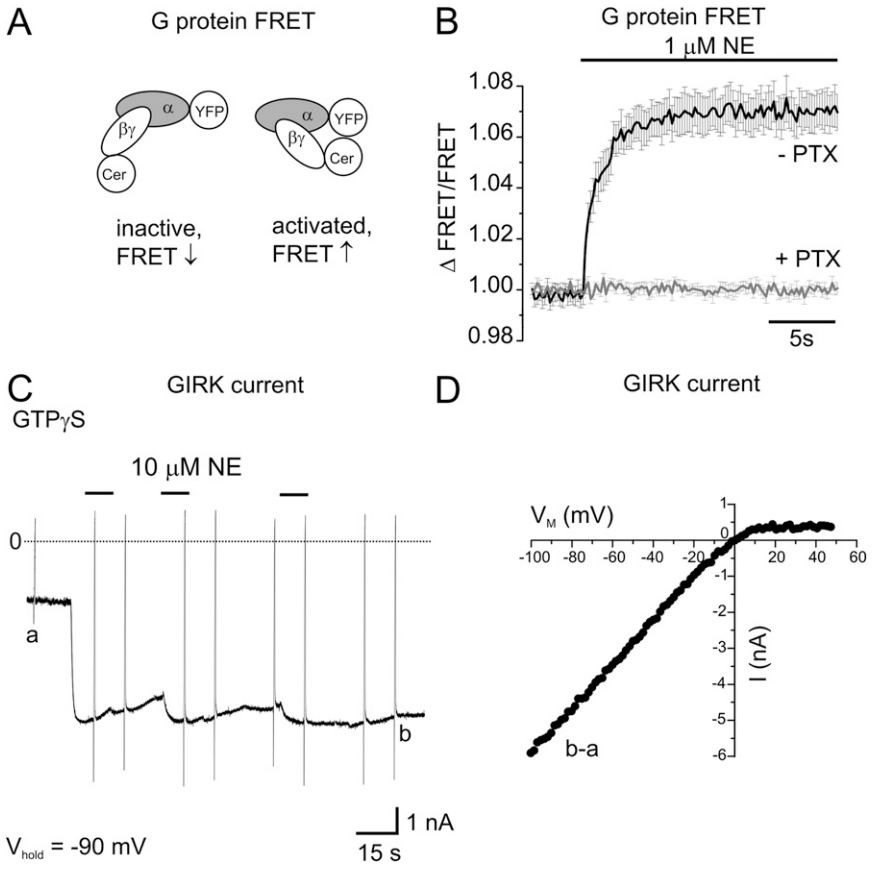

Fig. S2. Effective uncoupling of G_i proteins from the α_{2A}AR with pertussis toxin (PTX) or GTPγS. (*A*) Schematic representation of a FRET assay that uses a wild-type α_{2A}AR with fluorescently tagged G-protein subunits to directly report G_i protein activation (1). (*B*) Treatment with PTX (50 ng/mL for 3 to 5 h) effectively uncouples G_i proteins from the α_{2A}AR. The traces shown represent an average of 8 (−PTX) or 10 (+PTX) individual recordings (mean ± SEM). (*C*) Representative trace of a GIRK current from a HEK 239 cell expressing α_{2A}AR-cam and GIRK1/4 subunits loaded with 500 μM of the nonhydrolyzable GTP analog GTPγS via the patch pipette (loading time 3 min). Brief applications of NE as indicated caused irreversible activation of G_i proteins, yielding to sustained NE-independent activation of GIRK currents. Note that this experiment also demonstrates effective coupling of α_{2A}AR-cam to G_i proteins. (*D*) The background-substracted *I*/*V*-curve (b-a, obtained from the voltage ramps a and b, as indicated in *C*) shows strong inward rectification.

1. Bünemann M, Frank M, Lohse MJ (2003) Gi protein activation in intact cells involves subunit rearrangement rather than dissociation. *Proc Natl Acad Sci USA* 100(26):16077–16082.

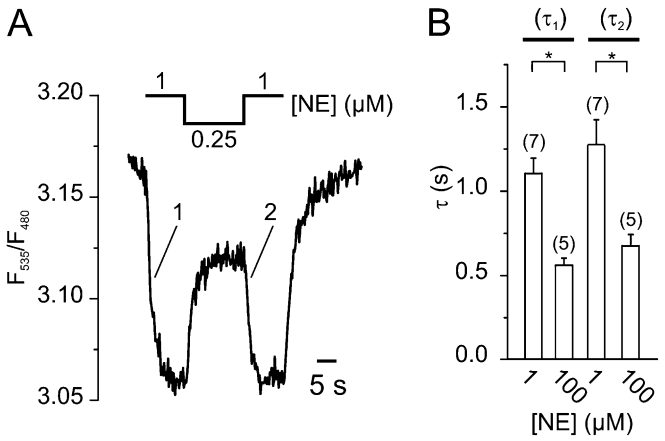

Fig. S3. Effect of different NE concentrations on the conformation of α_{2A}AR-cam. (*A*) Representative FRET response of a HEK 293 cell that was not subjected to voltage-clamp. Activation and deactivation of α_{2A}AR-cam was controlled by alternate application of high and low concentrations of NE. The time courses for initial activation (denoted as 1) and for reactivation upon agonist-switch (denoted as 2) were analyzed by calculating the corresponding τ-values τ_1 and τ_2. (*B*) Summarized data of τ_1 and τ_2 presented as mean ± SEM and analyzed with Student *t* test (initial binding: $^*P = 0.0010$; rebinding: $^*P = 0.0087$). Note that the observed changes in receptor conformation, caused by association (1 μM) and dissociation (250 nM) of NE, resemble the FRET signal observed with the voltage step protocol (Fig. 2*C*).

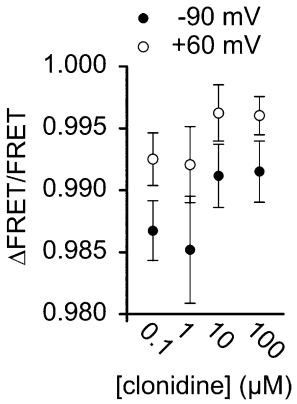

Fig. S4. Absolute FRET responses of clonidine-activated α_{2A}AR-cam. FRET amplitudes of HEK 293 cells expressing α_{2A}AR-cam were measured at −90 mV and at +60 mV as depicted in Fig. 3*B*. All cells displayed strong reduction in the FRET response at +60 mV, independent of the clonidine concentration that was used to activate the biosensor.

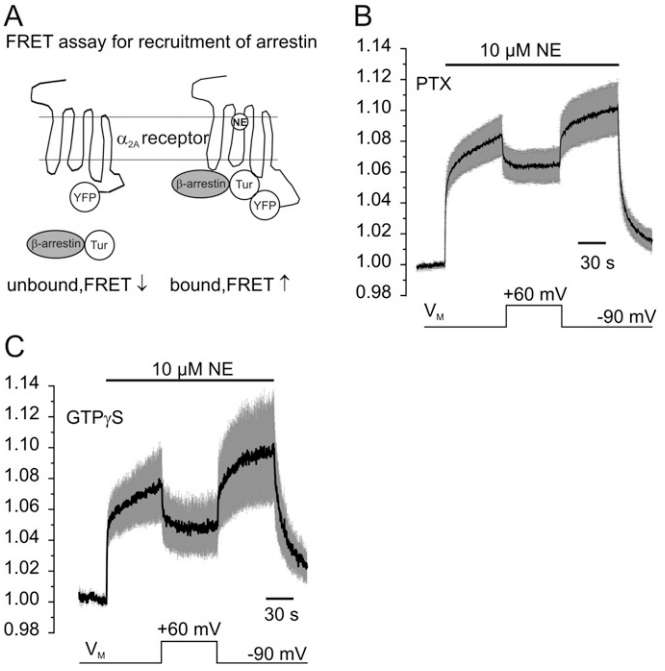

Fig. S5. Voltage-dependent recruitment of arrestin does not depend on G_i proteins. (*A*) Schematic representation of a FRET assay that uses α_{2A}AR-YFP and Turquiose-β-arrestin to report arrestin recruitment. (*B* and *C*) Application of NE at −90 mV resulted in a rise in the FRET signal, indicating binding of arrestin to the α_{2A}AR. Upon depolarization of the membrane, which deactivates the receptor, a reversible decrease of the FRET ratio (reflecting dissociation of arrestin from the receptor) was observed. This voltage dependence of α_{2A}AR-YFP was not dependent on G_i proteins, because it was not abolished in PTX-treated cells (*B*) or in cells that were loaded with GTPγS (*C*).